Reduction of *Pseudomonas aeruginosa* biofilm formation through the application of nanoscale vibration

Shaun N Robertson[1,2,3], Peter G Childs[2,4], Ayorinde Akinbobola[1], Fiona L Henriquez[5], Gordon Ramage[6], Stuart Reid[2,3], William G Mackay[1*], Craig Williams[1]

[1]Institute of Healthcare, Policy and Practice, School of Health & Life Sciences, University of the West of Scotland, High Street, Paisley PA1 2BE, Scotland, UK

[2]SUPA, Institute of Thin Films, Sensors and Imaging, School of Engineering and Computing, University of the West of Scotland, High Street, Paisley PA1 2BE, Scotland, UK

[3]SUPA, Department of Biomedical Engineering, University of Strathclyde, 40 George Street, Glasgow G1 1QE, Scotland, UK

[4]Centre for the Cellular Microenvironments (CeMi), School of Engineering, University of Glasgow, G12 8LT, Scotland, UK

[5]Institute of Biomedical and Environmental Health Research, School of Health & Life Sciences, University of the West of Scotland, High Street, Paisley PA1 2BE, Scotland, UK

[6]School of Medicine, Dentistry and Nursing, MVLS, University of Glasgow, 378 Sauchiehall St, Glasgow G2 3JZ, Scotland, UK

***Corresponding author**: William Gordon Mackay, Institute of Healthcare, Policy and Practice, School of Health & Life Sciences, University of the West of Scotland, High Street, Paisley PA1 2BE, Scotland, UK. Phone. +44 1418483000 Email: w.mackay@uws.ac.uk.

Keywords: Nanovibration, Biofilm formation, *Pseudomonas aeruginosa*, Extracellular matrix, Nanokicking, Mechanotransduction

Short title: *P. aeruginosa* biofilm and nanoscale vibration

Abstract: Bacterial biofilms pose a significant burden in both healthcare and industrial environments. With the limited effectiveness of current biofilm control strategies, novel or adjunctive methods in biofilm control are being actively pursued. Reported here, is the first evidence of the application of nanovibrational stimulation ("nanokicking") to reduce the biofilm formation of *Pseudomonas aeruginosa*. Nanoscale vertical displacements (approximately 60 nm) were imposed on *P. aeruginosa* cultures, with a significant reduction in biomass formation observed at frequencies between 200 to 4000 Hz at 24 h. The optimal reduction of biofilm formation was observed at 1 kHz, with changes in the physical morphology of the biofilms. Scanning electron microscope imaging of control and biofilms formed under nanovibrational stimulation gave indication of a reduction in extracellular matrix (ECM). Quantification of the carbohydrate and protein components of the ECM was performed and showed a significant reduction at 24 h at 1 kHz frequency. To model the forces being exerted by nanovibrational stimulation, laser interferometry was performed to measure the amplitudes produced across the Petri dish surfaces. Estimated peak forces on each cell, associated with the nanovibrational stimulation technique, were calculated to be in the order of 10 pN during initial biofilm formation. This represents a potential method of controlling microbial biofilm formation in a number of important settings in industry and medical related processes.

Introduction

It is estimated that over 80% of the world's microbial biomass exists in a biofilm state (1). These microbial biofilms represent the preferred mode of growth of bacteria, yeasts, filamentous fungi and protists (2, 3). A microbial biofilm can briefly be described as a consortium of cells enclosed in a self-derived extracellular polymeric substance (EPS), interspersed with water channels, and attached to a surface or each other (4, 5). This enclosed consortium of cells has a greater capacity to resist environmental stresses, and is important as a microbial survival strategy (6).

Clinically, the role of biofilms may have been underestimated, but recent guidance aims to correct this (7), as it has been estimated that biofilms account for between 65% and 75% of all infections (8, 9). The transition of planktonic cells to a biofilm community, confers with it a vastly increased tolerance to antibiotics (10) and disinfectants (11). As well as being a survival mechanism for microorganisms, it is possible that organisms growing within a biofilm may be more virulent. In blood stream infections a biofilm phenotype has been associated with a higher mortality rate in contrast to planktonic cells (12), possibly due to dispersal of cells from the biofilm (13). Biofilm studies investigating the capacity of clinical isolates to form biofilms have grouped strains of the same species into low and high biofilm formers, with the latter being shown to have an increased pathogenicity and resistance; this effect has been demonstrated in both bacteria (14, 15) and fungi (16).

Within the wider environment, biofilm formation can lead to food spoilage and contamination of food processes resulting in significant financial costs (17). Industrial processes that involve pipelines can suffer significant degradation over time due to microbial influenced corrosion. This is mediated by biofilm formation on the inner surface of the pipe, leading to fouling and corrosion of iron and steel alloys (18, 19).

It is well known that eukaryotic cells can respond to mechanical stress and convert these mechanical stimuli into an electrical or biochemical response, a process termed mechanotransduction (20). A recent review has highlighted the multitude of mechanical forces that bacteria can experience when attached to surfaces (21). Yet, our understanding of the response of bacteria to these mechanical forces is less well formed than that of eukaryotic cells. Existing studies have investigated microbial biofilm formation in response to surface acoustic waves induced vibration (22) and acoustic induced vibration (23). Surface acoustic waves induced vibration was effective in reducing the bacterial burden in Foley catheters whereas acoustic vibration was demonstrated to increase biofilm formation of *Pseudomonas aeruginosa* in Petri dishes.

The application of nanovibrational stimulation by use of the reverse piezo effect to control cell behaviour has been described in a recent review (24). Using this method, precise control of experimental parameters can be achieved which are independent of shear flow, produces negligible heat and minimises variability in the displacements applied across the surface of the Petri dishes (25). Nanovibrational stimulation has previously been applied to endothelial LEII cells (26) and mesenchymal stem cells (24-29). Here, we report the first study of nanovibrational stimulation on the formation of *P. aeruginosa* biofilms.

Materials and methods

Nanovibrational apparatus

The nanovibrational stimulation apparatus was nominally identical to that used by both Nikukar et al and Curtis et al (25, 26). To perform experiments with 35 mm Petri dishes, six aluminium support discs were cut to 32 mm diameter, 3 mm thickness, polished (to ensure a smooth bonding surface). Six 35 mm tissue culture treated polystyrene Petri dishes (Corning, UK) were bonded onto the six aluminium discs using Loctite 2-part epoxy (Loctite,

Hempstead, UK). Each cultureware assembly was subsequently bonded to a piezo transducer (model no. 010–05H Physik Instrumente, Karlsruhe/Palmbach, Germany) by application of a non-solvent glue (Bostik, UK). The transducers provided the required nanoscale amplitudes when driven by a continuous sine wave output from a GWINSTEK AFG-2005 arbitrary function generator (Good Will Instrument Euro B.V., Velhoven, Netherlands). The functionality of the piezo/cultureware assemblies was verified by incrementally driving each one at an audible frequency, i.e. 5 kHz, and listening to the audible output generated. The final set-up of the nanovibrational stimulation apparatus is shown in Figure 1.

Laser interferometry and force estimation

Nanoscale amplitudes were measured by laser interferometry as previously described (25). Measurements were taken at the centre and edge of 35 mm Petri dishes, measurements were performed on 3 separate Petri dishes. An estimation of the maximum force exerted due to nanovibrational stimulation was calculated as previously described (27). The average amplitudes measured at each frequency were used to calculate the maximum force exerted, as there were slightly variations in the amplitudes produced.

Culture conditions, standardisation and experimental conditions

P. aeruginosa type strain NCTC 10332 (*P. aeruginosa* 10332) was used for all work in this study. All working stocks of *P. aeruginosa* 10332 were maintained at 4°C on Lysogeny broth agar (Oxoid, Cambridge, UK). *P. aeruginosa* 10332 was propagated in Lysogeny broth (LB [Oxoid, Cambridge, UK]). *P. aeruginosa* 10332 was propagated in LB for 16 h at 37°C with shaking at 250 rpm. The culture was then washed by centrifugation (1,600 x *g*), resuspended in 1x phosphate buffered saline (PBS) twice then adjusted to an OD_{570nm} corresponding to 1 $x10^8$ CFU/mL. A working inoculum was prepared in LB broth at 1 $x10^5$ CFU/mL. Sterile LB (1 mL) was added to each Petri dish before addition of 1 mL of the *P. aeruginosa* 10332

inoculum, giving a final inoculum of 5 x10^4 CFU/mL. LB without addition of inoculum was used as a negative growth control. The nanovibrational stimulation apparatus was incubated at 37°C for 24 h in air, with the signal generator connected via crocodile clips to the piezo actuators terminal wires. In all experiments a driving potential of 20 V peak to peak (pk-pk) was used producing an approximately 60 nm displacement. Alteration of frequency was performed by changing the input frequency via the digital control panel of the function generator.

Quantifying biofilm biomass

Filtered crystal violet (CV [Fisher, UK]) was prepared to a 0.1% w/v solution in deionised water (dH_2O). At the experimental end time point the nanovibrational stimulation apparatus was removed from the incubator and the Petri dishes detached from the aluminium support discs. Once detached the supernatants were aspirated and the biofilm was washed twice with 1x PBS to remove non-adherent cells. One millilitre of 0.1% w/v CV was added to each Petri dish including the media-only control. Petri dishes were then incubated at room temperature for 15 min. Excess CV stain was removed by washing in dH_2O until subsequent washes did not remove any further excess staining. To quantify the bound CV, 80% v/v ethanol was added, and Petri dishes gently rocked to allow full solubilisation of the bound CV. This procedure was repeated for all experimental conditions, controls and media only control. To a 96 multi-well plate (Corning, UK), 100 µl of the solubilised CV was transferred from the Petri dish in triplicate. The 96 multi-well plate was then read at OD_{595nm} using an Infinite F200 Pro plate reader (Tecan Group Ltd, Switzerland).

Enumeration of colony forming units

At end point Petri dishes were removed from the aluminium disc and washed twice with 1x PBS. To disrupt the biofilm, 1 mL of 1x PBS was added to a petri dish and sealed with parafilm.

Sonication was performed for 10 min at 15 kHz, with subsequent disrupted and detached biofilm in 1x PBS transferred to a 1.5 mL Eppendorf tube. To ensure full disruption and detachment of the biofilm, the Petri dish was stained with CV, full disruption occurring when the CV staining of the Petri dish was negative. To enumerate the colony forming units (CFU) the Miles and Misra method was performed (30). Serial decimal dilutions were performed in 1x PBS and 20 µl plated on LB agar in triplicate for each dilution. LB agar plates were inverted and incubated at 37°C for 24 h, following which the CFU was calculated by counting the colonies at the easiest to count dilution (~20 – 60 colonies).

Live/dead biofilm imaging

Following test conditions Petri dishes were removed from aluminium discs, as previously described. Supernatant was aspirated, and biofilms washed twice with PBS. A live/dead staining solution was prepared using the LIVE/DEAD BacLight Bacterial Viability Kit for microscopy and quantitative assays (Invitrogen, UK). Briefly, 1 µl of SYTO9 and propidium iodide (PI) were added per 1 mL of dH_2O. To each Petri dish 1 mL of staining solution was added, Petri dishes were then incubated for 15 min in the dark at room temperature. The staining solution was aspirated, and the biofilm washed twice with dH_2O to halt any residual staining. Biofilms were imaged using an EVOS FL (Life Technologies, UK) all in one fluorescent microscope. Fluorescent images were obtained using the GFP (470/22, 510/42) and Texas Red (585/29, 624/40) lightcubes (Life Technologies).

SEM analysis

Biofilms with (1 kHz applied on inoculation) and without nanovibrational stimulation were grown for 24 h at 37°C as previously detailed. Biofilms were washed twice with 1x PBS and fixed with a 2% w/v para-formaldehyde, 2% v/v glutaraldehyde, 0.15 M sodium cacodylate, and 0.15% Alcian Blue (pH 7.4) solution, and prepared for SEM as described by Erlandsen et

al (31), with modification of counter staining process by addition of 1 mL 0.5% w/v uranyl acetate for 1 h, at room temperature in the dark. Following which, progressive dehydration steps were performed with increasing concentrations of ethanol (EtOH), twice for 5 min for each (30% v/v, 50% v/v, 70% v/v, and 90% v/v). Dehydration by absolute and dried absolute EtOH was performed 4x 5 min. Following dehydration steps, substrates were critically dried by addition of hexamethyldisilazane (HDMS) twice and stored in a desiccator overnight. Fixed and dried biofilms were sputter coated with 5 nm of gold using an EMSscope SC500 sputter coater (EMS, UK). Examination of samples was performed on a Hitachi S-4100 scanning electron microscope under vacuum, operated at 10 kV.

Quantification of ECM components

Biofilms with (1 kHz applied on inoculation) and without nanovibrational stimulation were grown for 24 h following which the supernatant was aspirated and biofilms were washed with 1x PBS twice to remove non-adherent cells. Biofilms were harvested in 1 mL 1x PBS and disrupted by scraping with a cell scraper. Biofilms samples were stored at –20°C for a maximum of 1 week prior to processing. Biofilms samples were fully thawed and homogenised by a combination of vortexing and pipetting. Biofilm samples were 0.2 µm filtered and the resultant eluent aliquoted into Eppendorf tubes. To measure the protein content of the biofilm samples the Bradford assay was performed (32) with bovine serum albumin as a standard. To measure the carbohydrate content of the biofilm samples, an optimised phenol-sulphuric acid method with glucose standards was performed (33).

Visualisation of potential lateral force production

To visualise any potential production of shear flow, 5 µl of dye composition (30% v/v glycerol, 0.25% w/v bromophenol blue and 0.25% w/v xylene cyanol), was added concurrently to 2 Petri dishes, with and without nanokicking. A time lapse video was

recorded of the dye dispersal, and the experiment repeated in triplicate. Videos were exported and converted to JPG stills using Paxillion Free Image converter software (Softonic, Barcelona, Spain). To quantify the dispersal of the dye, images at 10 s intervals were assessed for the diameter of dispersal in AxioVision V4.8 (Zeiss, Feldbach, Switzerland). Diameter measurements were taken in 4 aspects to average and account for non-uniform dispersal of the dye. Rate of dispersal was calculated at 10 s intervals over a time course of 0 – 100 s. Linear regression curve analysis was performed on the dispersion of a dye over time. Linear function lines were plotted when there was no significant difference between the control and nanokicking replicates.

Statistical analysis

All data were assessed for normality using a Shapiro–Wilk test. For assessing the statistical significance of the alteration of frequency and time of application of nanovibrational stimulation, a one-way ANOVA with Tukey *post hoc* correction was performed. For assessing the statistical significance of observed alteration of biofilm formation kinetic, comparison of CFUs and components of the biofilm matrix a student t-test was performed. In all experiments, statistical significance was achieved when $p < 0.05$. Data were exported from the Infinite F200 Pro plate reader to Microsoft Excel (Microsoft, Redmond, WA, USA). Assessment of normality, statistical analysis and plotting of data was performed in GraphPad Prism 7.0 (GraphPad Software Inc, San Diego, CA, USA).

Results

Laser interferometry and modelling of maximum force on *P. aeruginosa* cells

Validation of the cultureware assembly was quantified by measurement of the displacements generated by nanovibrational stimulation using a SIOS laser interferometer (Figure 2A). Displacement was observed to increase linearly with increased pk-pk voltage supplied. The theoretical force exerted by the nanovibrational stimulation on a single *P. aeruginosa* cells

can be mathematical calculated using Newton's second law, that of force (F) being determined by the mass (m) times acceleration (a) (26, 27). In this case the mass refers to the column of fluid directly above each cell, with the peak acceleration being $A_0(2\pi f)^2$, where f is frequency and A_0 is the vibration amplitude (note that this is half of the total peak to peak displacement). An estimate for this mass is determined by the average surface area of a *P. aeruginosa* cell being 1 µm x 5 µm, with an aqueous column of culture media extending 2 mm above (with the density of water used to calculate this mass). Peak values due to acceleration during vibration are calculated as described in the papers by Curtis et al and Nikukar et al (26, 27). Figure 2B shows the modelled peak force exerted per single cell of *P. aeruginosa* due to nanovibrational stimulation at frequencies of 100, 200, 400, 500, 1000, 2000 and 4000 Hz with a 20 V pk - pk driving potential. Peak forces of 0.4 pN, 1.9 pN, 2.9 pN, 11.7 pN, 42.9 pN and 133.5 pN were calculated.

Effect of altering the frequency and time of application of nanovibrational stimulation on *P. aeruginosa* biofilm formation

Previous literature has demonstrated that vibrating a surface can alter biofilm formation (23). A range of frequencies from 10 Hz to 4 kHz was examined to determine if nanovibrational stimulation alters *P. aeruginosa* biofilm formation. No reduction in biomass at 24 h was observed at frequencies of 10 and 100 Hz ($p > 0.05$) (Figure 3A). A statistically significant reduction in biomass was observed at 24 h, at frequencies of 200 Hz, 400 Hz, 500 Hz, 1 kHz, 2 kHz and 4 kHz (52.5%, 52.8%, 54.0%, 64.0%, 41.6% and 38.9% reduction respectively, $p < 0.001$ one-way ANOVA with Tukey post hoc test).

It was noted that the reduction in biomass was less at frequencies of 2 and 4 kHz compared to 1 kHz, with the reduction at 4 kHz being significantly lower than that of 1 kHz ($p < 0.05$). The greatest reduction of biomass was observed at 1 kHz, while not significantly different to

the frequencies of 200 Hz, 400 Hz and 500 Hz, it was consistently lower in all biological replicates. Due to limitations of the equipment (limited number of Petri dishes and set-up time) it was decided to focus on one frequency; therefore, a frequency of 1 kHz was selected for further investigation.

Biofilm formation has defined temporal stages initiated from the initial reversible attachment, following which irreversible attachment occurs and ultimately biofilm formation and maturation. To determine if the time of application of the nanovibrational stimulation after inoculation influenced biofilm formation, nanovibrational stimulation was applied continuously at 1 kHz from 0, 2, 4 and 6 h after initial inoculation for a total time of 24 h, e.g. 0 h equals 24 h stimulation, 2 h equals 2 h no stimulation and 22 h stimulation. When nanovibrational stimulation was applied from 0 h and 2 h, a significant reduction in the measured biomass at 24 h was observed when compared to the control (50.8% and 57.5%) (one-way ANOVA with Tukey post hoc test, $p < 0.001$; Figure 3B). Application of nanovibrational stimulation from 4 h and 6 h after inoculation resulted in no significant reduction in total biofilm formation when compared to control (one-way ANOVA with Tukey post hoc test, $p > 0.05$).

Effect of nanovibrational stimulation on development kinetic of *P. aeruginosa* biofilm

To better understand the observed reduction in biomass at 24 h and the dependence on the time of application of the nanovibrational stimulation, biomass formation kinetics for *P. aeruginosa* 10332 was performed. Biomass was assessed using the CV biomass assay at 0, 2, 4, 6, 12, and 24 h with and without nanovibrational stimulation at 1 kHz frequency, 30 nm amplitude applied 0 h after inoculation. At 2 h, there was no significant difference between the stimulated *P. aeruginosa* 10332 and control, but at 4 h *P. aeruginosa* subjected to nanovibrational stimulation showed a significantly lower biomass at OD_{595nm} compared with

non-stimulated control of 0.3 and 1 (un-paired Student T-test, $p < 0.05$; Figure 4). Without nanovibrational stimulation the exponential formation of the bacterial biofilm continued to 12 h and plateaued by 24 h reaching a final average OD_{595nm} of 3.27. With nanovibrational stimulation, exponential biomass formation was not observed through the course of the experiment. At 24 h the biomass was significantly lower at an average OD_{595nm} of 0.94 (un-paired Student T-test, $p < 0.001$).

Nanovibrational stimulation does not reduce the number of cells in the biofilm and planktonic phase

Due to the nature of the CV assay, cells and extracellular matrix are both stained by CV, in addition if there is a lower number of cells adhered to the surface, a lower quantity of extracellular matrix may be produced. To investigate if the reduction in biomass was due to a reduction in the number of cells in the biofilm, Miles and Misra counts were performed to enumerate the number of CFUs. In addition, to determine if nanovibrational stimulation could cause dislodgement of cells from the surface, the planktonic CFU was also investigated. No statistically significant reduction in the CFU/cm^2 was noted ($p > 0.05$) between the control (1.62×10^9 CFU/cm^2) and stimulated (1 kHz) biofilm (7.99×10^8 CFU/cm^2) (Figure 5) at 24 h. There was a mean 10-fold increased recovery of planktonic *P. aeruginosa* when comparing the control (6.94×10^{10} CFU/mL) versus stimulated (6.88×10^9 CFU/mL), however this was not statistically significant ($p = 0.3648$). To determine if there was a difference in the total recovered CFU, the planktonic and sessile CFU recovery were combined. This gave a total recovery of 1.46×10^{10} CFU for the control and 8.44×10^{10} CFU for the stimulated, this difference was not statistically significant ($p = 0.5522$, unpaired Student T-test).

Microscopic examination of the effect of nanovibrational stimulation on *P. aeruginosa* biofilm architecture

As no statistically significant reduction in cells numbers was noted, live/dead staining was performed on 24 h biofilms with and without the application of nanovibrational stimulation to

visualise the biofilm. Biofilms formed under nanovibrational stimulation at 1 kHz showed a change in structural architecture and density compared to the control (Figure 6A and B). With increased magnification it was shown that there were regions of sparse microbial coverage compared to the controls (Figure 6C). When the number of dead cells was assessed using PI staining, no significant difference ($p > 0.05$) was observed between the control and stimulated biofilms (supplementary table S1). During visual examination of the 1 kHz stimulated biofilms, striated line-like formations were visible; these were interspersed variably across the biofilms, yet they were observed in all technical and biological independent replicates with 1 kHz nanovibrational stimulation. Representative image is shown in Figure 6B and C. When propidium iodide staining was viewed, staining was observed that was concordant with lines observed with the SYTO9 live cell staining (Figure 6B and C PI staining), however this did not appear to be stained cells. Collectively, these observations provide visual evidence of an alteration in the biofilm formation structure due to the 1 kHz nanovibrational stimulation when compared to the control.

To further visualise the altered biofilm formation of *P. aeruginosa* and the lower biomass due to nanovibrational stimulation, scanning electron microscopy was performed. Control biofilms had confluent growth with microcolonies evident across the Petri dish surface with ECM being visible, (albeit in a dehydrated state due to the ethanol dehydration method used to prepare the samples) (Fig. S1). Comparison of the control biofilms (Figure 7A & B) versus the 1 kHz biofilms (Figure 7C & D) showed a similar pattern of confluence across the Petri dish surface with a higher confluence in the middle and a lower confluence at the edge. In keeping with the fluorescent imaging, regions of lower density of cells was observed in 1 kHz nanovibrational stimulated biofilms compared to the control (Figure 7A & C).

Nanovibrational stimulation reduces key matrix components of the ECM of *P. aeruginosa* biofilms

The reduction in biomass coupled with visual evidence of an altered biofilm structure gives tentative evidence that the ECM produced by *P. aeruginosa* biofilms is reduced due to the nanovibrational stimulation at 1 kHz. To further investigate this hypothesis, quantification of the carbohydrate and protein components of *P. aeruginosa* 10332 biofilms with and without nanovibrational stimulation was performed. The average protein content of the control biofilms was 19.62 μg/cm^2, the average protein content of stimulated biofilms was 6.78 μg/cm^2 equating to a 65.4% reduction which was statistically significant ($p < 0.0001$) (Figure 8). The average carbohydrate content of the control biofilms was 8.42 μg/cm^2, the average carbohydrate content of stimulated biofilms was 2.96 μg/cm^2, equating to a 64.8% reduction which was statistically significant ($p < 0.0001$) (Figure 7).

Discussion

This is the first reported demonstration of a reduction in bacterial biofilm formation due to an induction of a vertical nanoscale vibration approximately 30 nm amplitude, at a frequency of 200 Hz – 4 kHz, when applied 0-2 h after inoculation. Biofilm formation can be grouped into a number of key stages: reversible adhesion, irreversible adhesion, proliferation, ECM production and ultimately formation of a mature biofilm (34). The optimal time of application of the nanovibrational stimulus may give an indication that vibration at the nanoscale interferes with the initial attachment of *P. aeruginosa* 10332, as these time periods are known to be within the reversible period of cell attachment to a surface in the current model of biofilm development (34, 35). This would also indicate that the frequencies studied would be ineffective in disrupting pre-formed biofilms. Nanovibrational stimulation, however, cannot completely abrogate the adhesion of *P. aeruginosa* as biofilm growth occurs throughout the 24 h growth period, yet the final biomass at 24 h is significantly lower than the controls,

316 suggesting an additional effect to reduction of initial adherence. Initial surface interactions
317 have recently been demonstrated to be mediated by the mechanical activity of type IV pili
318 (TFP) in *P. aeruginosa* on short time scales (36). Persat and colleagues (36) have proposed a
319 molecular model for the surface sensing by TFP, whereby the cell encounters the surface and
320 through attachment and retraction of the TFP, tension is exerted on the TFP, this then
321 activates the Chp system, leading to cyclic adenosine monophosphate (cAMP) synthesis
322 within the first hour of attachment. TFP retraction forces have been measured to be within the
323 pN range (37), this is within the order of the forces generated by the nanovibrational
324 stimulation at a frequency of 1 kHz (approximately 10 pN) (Figure 2). While the forces
325 generated are of the same magnitude it is too early to establish a link between the forces
326 exerted by nanovibrational stimulation and an interaction with the tension forces exerted by
327 TFP.

328 Prior studies using shear flow have demonstrated altered biofilm phenotypes in *P. aeruginosa*
329 PA01 (38). Turbulent flow resulted in the formation of the streamlined patches that in some
330 cases had ripple-like structures perpendicular to the flow. The intersecting and crossing lines
331 observed (Figure 6) were different to the ripple-like formations produced by turbulent flow in
332 the PA01 study. It is of note that no statistically significant reduction in viable cells with the
333 Live/Dead staining was observed between the stimulated and unstimulated biofilms.
334 Exopolysaccharides have previously been shown to play an important role in biofilm
335 formation and structure (39). In this study, carbohydrate and protein content of the *P.*
336 *aeruginosa* 10332 biofilms were significantly reduced due to nanovibrational stimulation at 1
337 kHz. These data give strong indication that the reduction in biomass due to nanovibrational
338 stimulation is as a direct result of a reduction in the carbohydrate and protein content of the
339 biofilm matrix.

Acoustic stimulation provided by a speaker has previously been shown to enhance biofilm formation in response to non-uniform micrometre displacements (23). This stimulation method may have promoted accelerated biofilm formation due to clustering of the *P. aeruginosa* at early time points (concentric rings) leading to potentially higher levels of quorum sensing molecules. In contrast, our results have shown that uniform nanometre scale displacements result in decreased biofilm formation. This may indicate that biofilm formation can be controlled by the uniformity of the stimulation thereby allowing variable control of biofilm formation dependent on the application *e.g.* it may be beneficial to promote biofilm growth for bio-engineering purposes. A proposed hypothesis of how nanovibrational stimulation reduces biofilm formation is that of initial inhibition/delaying of the adherence of *P. aeruginosa* leading to a reduced quantity of extracellular components of the biofilm being produced *e.g.* delayed attachment leading to a less mature biofilm when compared to the control. It is yet undetermined if molecular mechanisms play a role in this observed mechanism of biofilm reduction.

A number of possible confounding factors have also been considered and discounted. It has previously been demonstrated that the rapid expansion and contraction of the piezo ceramic generates negligible heat transfer to the aluminium disc upon which the Petri dish sits (25, 28). This means that the effect is unlikely to be due to heating of the culture system (Fig. S2). Shear force mediated effects on adhesion have also been demonstrated in *P. aeruginosa* (40). However, our experimental design minimises the generation of any shear flow by minimising lateral motion of the media, only vertical movement is observed (Fig. S3). The uses of an aluminium disc and Petri dish ensures rigidity and minimises any differential vibration amplitudes, which could also induce shear flow across the growth surface at a frequency of 1 kHz and 30 nm amplitude.

In conclusion, we have described a novel method of biofilm control using piconewton forces that does not require the use of antibiotics or other chemical agents. This negates the potential for traditional environmental drug resistance mechanisms that have been shown to translate into clinical treatment failures (41, 42). This effect may have a number of potential applications in combating biofilms in the industrial setting and healthcare setting, but further work is required to fully understand the mechanisms by which nanovibrational stimulation causes this effect.

Acknowledgments

The authors would like to thank Professor Harry Staines for useful statistical discussion and his interest in this work. We thank Dr Liz Porteous for her assistance in SEM imaging. We also thank Jim Orr for laboratory assistance. We also would like to thank Professor Matthew Dalby for his proof reading of this manuscript. We are grateful for the financial support provided by BBSRC (BB/N012690/1), EPSRC (EP/N012631/1), STFC, SUPA, the Royal Society, NHS Greater Glasgow and Clyde, and the University of the West of Scotland. SNR, WGC & CW designed all experiments, SNR performed all experimental work. PGC provided support with the nanovibrational apparatus. AA provided assistance with biofilm component experimental work. All figures were produced by SNR. Manuscript was written through contributions of SNR, PGC, FLH, GR, SR, WGC & CW. All authors have given approval to the final version of the manuscript. Funding sources played no role in the following: design of this study, collection of data, analysis of data, interpretation of data and writing of the report. The authors declare no competing financial interests. The datasets generated are available from the corresponding author on reasonable request.

References:

1. **Beikler, T. and Flemmig, T. F.:** Oral biofilm-associated diseases: trends and implications for quality of life, systemic health and expenditures, Periodontol 2000., **55**, 87 - 103 (2000).

2. **Hall-Stoodley, L., Costerton, J. W., and Stoodley, P.:** Bacterial biofilms: from the Natural environment to infectious diseases, Nat Rev., **2**, 95 - 108 (2004).

3. **Siqueira, V. M. and Lima, N.:** Biofilm formation by filamentous fungi recovered from a water system, J Mycol., **2013**, 9 (2013).

4. **de Beer, D., Stoodley, P., Roe, F., and Lewandowski, Z.:** Effects of biofilm structures on oxygen distribution and mass transport, Biotechnol Bioeng., **43**, 1131 - 1138 (1994).

5. **Lawrence, J. R., Korber, D. R., Hoyle, B. D., Costerton, J. W., and Caldwell, D. E.:** Optical sectioning of microbial biofilms, J Bacteriol., **173**, 6558-6567 (1991).

6. **Davey, M. E. and O'Toole, G. A.:** Microbial biofilms: from ecology to molecular genetics, Microbiol Mol Biol Rev., **64**, 847-867 (2000).

7. **Høiby, N., Bjarnsholt, T., Moser, C., Bassi, G. L., Coenye, T., Donelli, G., Hall-Stoodley, L., Holá, V., Imbert, C., Kirketerp-Møller, K., and other 5 authors:** ESCMID∗ guideline for the diagnosis and treatment of biofilm infections 2014, Clin Microbiol Infect., **21**, S1-S25 (2015).

8. **Bryers, J. D.:** Medical biofilms, Biotechnol Bioeng., **100**, 1-18 (2008).

9. **Davies, D.:** Understanding biofilm resistance to antibacterial agents, Nat Rev Drug Discov., **2**, 114-122 (2003).

10. **Høiby, N., Bjarnsholt, T., Givskov, M., Molin, S., and Ciofu, O.:** Antibiotic resistance of bacterial biofilms, Int J Antimicrob Agents., **35**, 322-332 (2010).

11. **Bridier, A., Briandet, R., Thomas, V., and Dubois-Brissonnet, F.:** Resistance of bacterial biofilms to disinfectants: a review, Biofouling., **27**, 1017-1032 (2011).

12. **Tumbarello, M., Posteraro, B., Trecarichi, E. M., Fiori, B., Rossi1, M., Porta, R., de Gaetano Donati, K., La Sorda, M., Spanu, T., Fadda, G., Cauda, R., and Sanguinetti, M.:** Biofilm production by *Candida* species and inadequate antifungal therapy as predictors of mortality for patients with candidemia, J Clin Microbiol., **45**, 1843 - 1850 (2007).

13. **Uppuluri, P., Chaturvedi, A. K., Srinivasan, A., Banerjee, M., Ramasubramaniam, A. K., Kohler, J. R., Kadosh, D., and Lopez-Ribot, J. L.:** Dispersion as an important step in the *Candida albicans* biofilm developmental cycle, PLoS Pathog., **6**, e1000828 (2010).

14. **Cha, J. O., Yoo, J. I., Yoo, J. S., Chung, H. S., Park, S. H., Kim, H. S., Lee, Y. S., and Chung, G. T.:** Investigation of biofilm formation and its association with the molecular and clinical characteristics of methicillin-resistant *Staphylococcus aureus*, Osong Public Health Res Perspect., **4**, 225-232 (2013).

15. **Sanchez, C. J. Jr., Mende, K., Beckius, M. L., Akers, K. S., Romano, D. R., Wenke, J. C., and Murray, C. K.:** Biofilm formation by clinical isolates and the implications in chronic infections, BMC Infect Dis., **13**, 47 (2013).

16. **Sherry, L., Rajendran, R., Lappin, D. F., Borghi, E., Perdoni, F., Falleni, M., Tosi, D., Smith, K., Williams, C., Jones, B., Nile, C. J., and Ramage, G.:** Biofilms formed by *Candida albicans* bloodstream isolates display phenotypic and transcriptional heterogeneity that are associated with resistance and pathogenicity, BMC Microbiol., **14**, 1-14 (2014).

17. **Van Houdt, R. and Michiels, C. W.:** Biofilm formation and the food industry, a focus on the bacterial outer surface, J Appl Microbiol., **109**, 1117-1131 (2010).

18. **Schwermer, C. U., Lavik, G., Abed, R. M., Dunsmore, B., Ferdelman, T. G., Stoodley, P., Gieseke, A., and de Beer, D.:** Impact of nitrate on the structure and function of bacterial biofilm communities in pipelines used for injection of seawater into oil fields, Appl Environ Microbiol., **74**, 2841-2851 (2008).

19. **Lenharta, T. R., Duncana, K. E., Beecha, I. B., Sunnera, J. A., Smitha, W., Bonifaya, V., Biria, B., and Suflitaa, J. M.:** Identification and characterization of microbial biofilm communities associated with corroded oil pipeline surfaces, Biofouling., **30**, 823-835 (2014).

20. **Martinac, B.:** Mechanosensitive ion channels: molecules of mechanotransduction, J Cell Sci., **117**, 2449-2460 (2004).

21. **Persat, A., Nadell, C. D., Kim, M. K., Ingremeau, F., Siryaporn, A., Drescher, K., Wingreen, N. S., Bassler, B. L., Gitai, Z., and Stone, H. A.:** The mechanical world of bacteria, Cell., **161**, 988-997 (2015).

22. **Hazan, Z., Zumeris, J., Jacob, H., Raskin, H., Kratysh, G., Vishnia, M., Dror, N., Barliya, T., Mandel, M., and Lavie, G.:** Effective prevention of microbial biofilm formation on medical devices by low-energy surface acoustic waves, Antimicrob Agents Chemother., **50**, 4144-4152 (2006).

23. **Murphy, M. F., Edwards, T., Hobbs, G., Shepherd, J., and Bezombes, F.:** Acoustic vibration can enhance bacterial biofilm formation, J Biosci Bioeng., **122**, 765-770 (2016).

24. **Childs, P. G., Boyle, C. A., Pemberton, G. D., Nikukar, H., Curtis, A. S., Henriquez, F. L., Dalby, M. J., and Reid, S.:** Use of nanoscale mechanical stimulation for control and manipulation of cell behaviour, Acta Biomater., **34**, 159-168 (2016).

25. **Nikukar, H., Reid, S., Tsimbouri, P. M., Riehle, M. O., Curtis, A. S., and Dalby, M. J.:** Osteogenesis of mesenchymal stem cells by nanoscale mechanotransduction, ACS Nano., **7**, 2758-2767 (2013).

26. **Curtis, A. S., Reid, S., Martin, I., Vaidyanathan, R., Smith, C. A., Nikukar, H., and Dalby, M. J.:** Cell interactions at the nanoscale: piezoelectric stimulation, IEEE Trans Nanobiosci., **12**, 247-254 (2013).

27. **Nikukar, H., Childs, P. G., Curtis, A. S. G., Martin, I. W., Riehle, M. O., Dalby, M. J., and Reid, S.:** Production of nanoscale vibration for stimulation of human mesenchymal stem cells, J Biomed Nanotechnol., **12**, 1478-1488 (2016).

28. **Pemberton, G. D., Childs, P., Reid, S., Nikukar, H., Tsimbouri, P. M., Gadegaard, N., Curtis, A. S., and Dalby, M. J.:** Nanoscale stimulation of osteoblastogenesis from mesenchymal stem cells: nanotopography and nanokicking, Nanomedicine (Lond)., **10**, 547-560 (2015).

29. **Tsimbouri, P. M., Childs, P. G., Pemberton, G. D., Yang, J., Jayawarna, V., Orapiriyakul, W., Burgess, K., González-García, C., Blackburn, G., Thomas, D., and other 6 authors:** Stimulation of 3D osteogenesis by mesenchymal stem cells using a nanovibrational bioreactor, Nat Biomed Eng., **1**, 758-770 (2017).

30. **Miles, A. A., Misra, S. S., and Irwin, J. O.:** The estimation of the bactericidal power of the blood, J Hyg (Lond)., **38**, 732-749 (1938).

31. **Erlandsen, S. L., Kristich, C. J., Dunny, G. M., and Wells, C. L.:** High-resolution visualization of the microbial glycocalyx with low-voltage scanning electron microscopy: dependence on cationic Dyes, J Histochem Cytochem., **52**, 1427-1435 (2004).

32. **Bradford, M. M.:** A rapid and sensitive method for the quantitation of microgram quantities of protein utilizing the principle of protein-dye binding, Anal Biochem., **72**, 248-254 (1976).

33. **Masuko, T., Minami, A., Iwasaki, N., Majima, T., Nishimura, S.-I., and Lee, Y. C.:** Carbohydrate analysis by a phenol–sulfuric acid method in microplate format, Anal Biochem., **339**, 69-72 (2005).

34. **Bordi, C. and de Bentzmann, S.:** Hacking into bacterial biofilms: a new therapeutic challenge, Ann Intensive Care., **1**, 1-19 (2011).

35. **Rasamiravaka, T., Labtani, Q., Duez, P., and El Jaziri, M.:** The formation of biofilms by *Pseudomonas aeruginosa*: a review of the natural and synthetic compounds interfering with control mechanisms, Biomed Res Int., **2015**, 759348 (2015).

36. **Persat, A., Inclan, Y. F., Engel, J. N., Stone, H. A., and Z., G.:** Type IV pili mechanochemically regulate virulence factors in *Pseudomonas aeruginosa*, Proc Natl Acad Sci U.S.A., **112**, 7563–7568 (2015).

37. **Maier, B., Potter, L., So, M., Long, C. D., Seifert, H. S., and Sheetz, M. P.:** Single pilus motor forces exceed 100 pN, Proc Natl Acad Sci U.S.A., **99**, 16012-16017 (2002).

38. **Purevdorj, B., Costerton, J. W., and Stoodley, P.:** Influence of hydrodynamics and cell signaling on the structure and behavior of *Pseudomonas aeruginosa* biofilms, Appl Environ Microbiol., **68**, 4457-4464 (2002).

39. **Ghafoor, A., Hay, I. D., and Rehm, B. H.:** Role of exopolysaccharides in *Pseudomonas aeruginosa* biofilm formation and architecture, Appl Environ Microbiol., **77**, 5238-5246 (2011).

40. **Lecuyer, S., Rusconi, R., Shen, Y., Forsyth, A., Vlamakis, H., Kolter, R., and Stone, H. A.:** Shear stress increases the residence time of adhesion of *Pseudomonas aeruginosa*, Biophys J., **100**, 341-350 (2011).

41. **Forsberg, K. J., Reyes, A., Wang, B., Selleck, E. M., Sommer, M. O., and Dantas, G.:** The shared antibiotic resistome of soil bacteria and human pathogens, Science., **337**, 1107-1111 (2012).

42. **Howard, S. J. and Arendrup, M. C.:** Acquired antifungal drug resistance in *Aspergillus fumigatus*: epidemiology and detection, Med Mycol., **49 Suppl 1**, S90-95 (2011).

Figure 1 – Nanovibrational stimulation apparatus. Example of a typical set-up with 35mm diameter Petri dishes attached. The Petri dish is mounted on an aluminium disc, which provides support to the Petri dish allowing uniform displacement across the entire surface area. The Petri dish with aluminium disc is then attached to the piezo then to the large aluminium block underneath, this ensures that the expansion of the piezo results in upwards movement of the Petri dish.

Figure 2 – Amplitude response to driving potential and frequency with peak force estimation. (A) Petri dish amplitude as a function of piezo driving potential. Interferometry was performed at a range of frequencies measured at the surface of the Petri dish. Measured amplitudes were linearly correlated to driving potential (B) The maximum force exerted due to acceleration as a result of nanovibrational stimulation was calculated using Newton's second law, based on the maximum amplitude measured by interferometry for each frequency, calculated from interferometry data. Data are mean ± SD, n = 3.

Figure 3 – *P. aeruginosa* biomass formation is dependent on both frequency and time of application of nanovibrational stimulation. (A) The effect of altering the frequency of the nanovibrational stimulus was performed and the resultant final biomass at 24 h was quantified by CV assay. Frequencies of 200 Hz through to 4 kHz were effective in reducing biomass formation at 24 h. (B) Nanovibrational stimulation at 1 kHz was applied at specified periods after inoculation (0, 2, 4 and 6 h) as indicated on the graph. Resultant biomass at 24 h was quantified by CV assay. A significant reduction in biomass formed was observed when nanovibrational stimulation was applied at 0 and 2 h post inoculation but not at 4 and 6 h port inoculation. Data are mean ± SD. One-way ANOVA with Tukey post hoc test, *** $p < 0.001$, * $p < 0.05$, n = 3.

Figure 4 - Biofilm formation kinetic of *P. aeruginosa* 10332 with (dashed) and without nanovibrational stimulation. *P. aeruginosa* 10332 was inoculated in LB broth at 5 x 10^4 CFU/mL and 2 mL seeded to each Petri dish on the nanokicking set-up. Nanokicking set-up was incubated at 37°C for 24 h. A Petri dish was removed at the respective time points, washed with 1x PBS, and crystal violet staining performed. Bound CV was desaturated with 80% v/v ethanol and 100 µl transferred to a 96 well flat bottom microtitre plate (n = 6). Data are mean ± SD. Unpaired Student T-test, * $p < 0.05$, ** $p < 0.01$, *** $p < 0.001$, n = 3.

Figure 5 – Microbial count determination disrupted biofilm and supernatants. Nanovibrational stimulation at a frequency of 1 kHz was applied after inoculation (0 h). Biofilms were disrupted by combination of sonication and cell scraping. Disrupted biofilm was resuspended in 1 mL PBS and Miles and Misra CFU counts performed. Resultant CFU/mL for biofilms were then adjusted to CFU/cm^2. Circle = Control, Square = stimulated 1 kHz. Data are mean ± SD, n = 3.

Figure 6 – Nanovibrational stimulation alters *P. aeruginosa* 10332 biofilm architecture. Representative images obtained on EVOS® FL all in one microscope. Syto9 (green - live) and PI (dead - red) images obtained at same fluorescent intensity and combined (merged). (A) Unstimulated controls, scale bar = 400 µm (B) 1 kHz stimulation non-uniform biofilm formation was observed, scale bar 400 µm (C) 1 kHz stimulation, unusual biofilm features were observed, Scale Bar = 200 µm.

Figure 7 – SEM evaluation of control and 1 kHz nanovibrational stimulated *P. aeruginosa* 10332 biofilms. Representative SEM images of *P. aeruginosa* 10332. Control biofilm (A) centre of Petri dish and (B) edge of Petri dish. Nanovibrationally stimulated biofilm (1 kHz) (C) centre of Petri dish, (D) edge of Petri dish. Scale Bar = 10 µm.

Figure 8 – Nanovibrational stimulation significantly reduces the protein and carbohydrate content of *P. aeruginosa* biofilm ECM. Quantification of protein and carbohydrate content of control and stimulated (1 kHz) *P. aeruginosa* biofilms performed by Bradford assay and phenol-sulfuric acid assay respectively. Data are mean ± SD, *** $p < 0.0001$, n = 3.

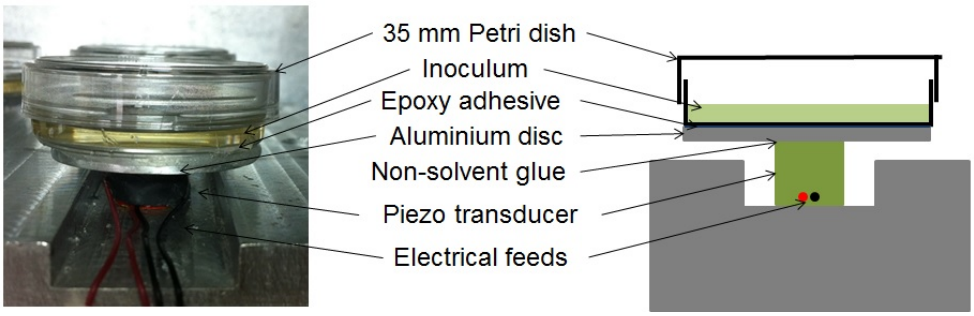

572
573 **Figure 1**
574
575

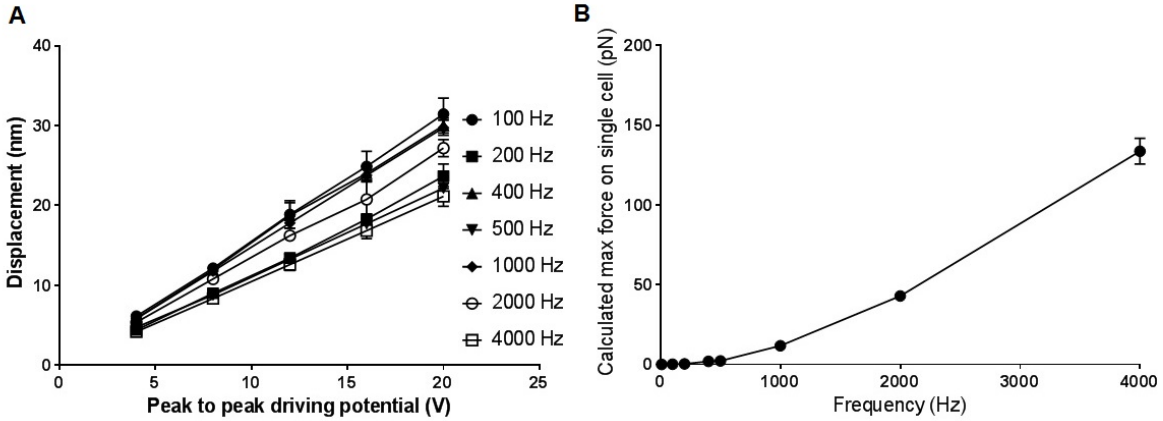

576
577 **Figure 2**

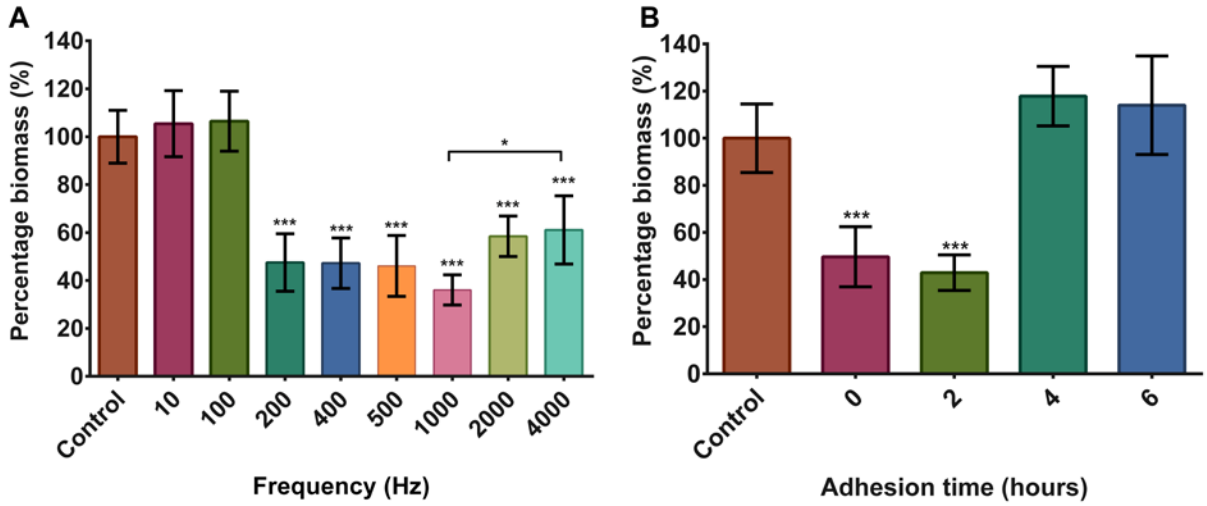

578
579 **Figure 3**
580

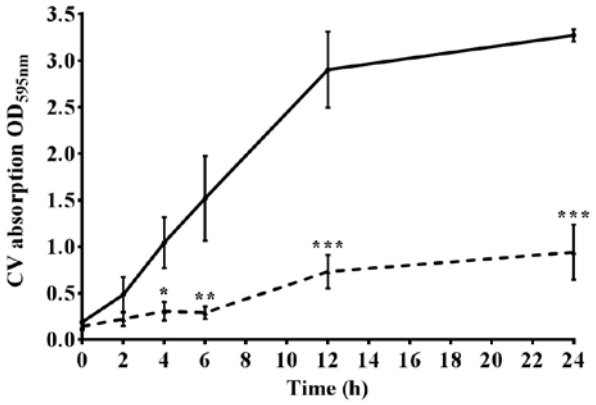

Figure 4

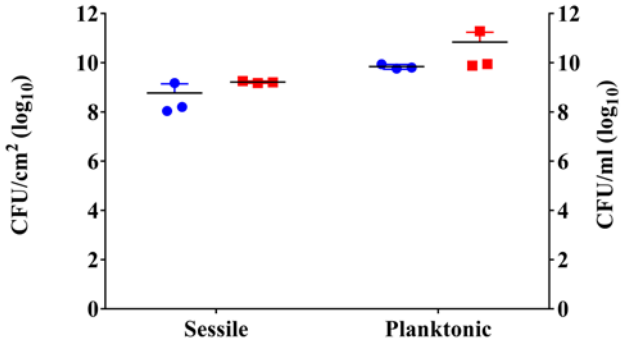

Figure 5

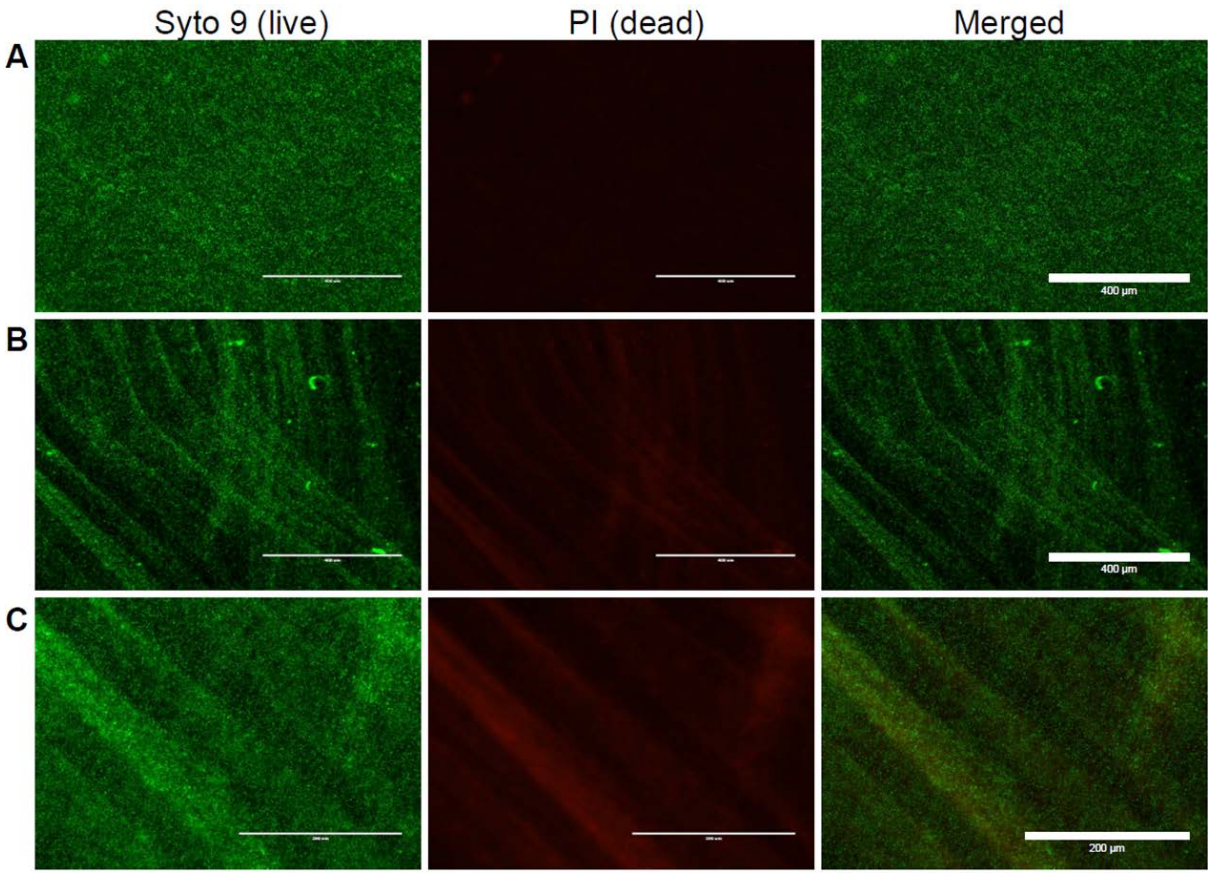

Figure 6

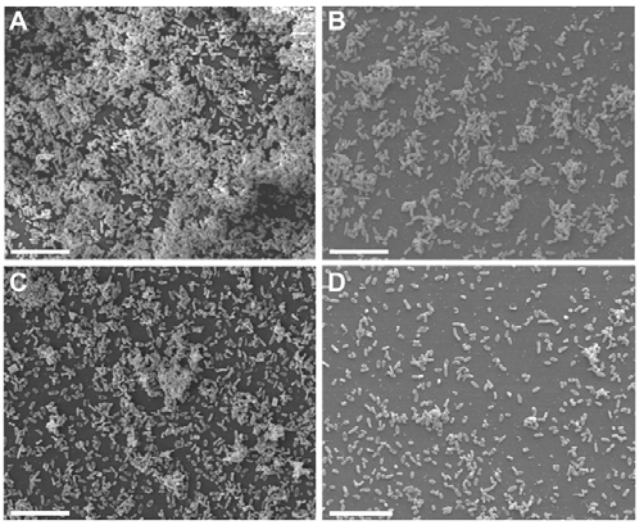

Figure 7

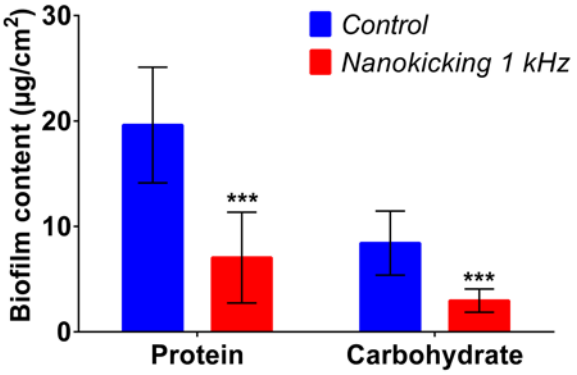
Biofilm content (µg/cm²)
30
20
10
0
Control
Nanokicking 1 kHz
***
***
Protein
Carbohydrate

Figure 8